Chapter 1

Introduction and Literature Survey

This chapter provides information about the motivation and origin of this thesis. The scope, structure and objectives of the thesis are defined followed by a brief introduction to graphite and aerosol. The characteristics of graphite, the parameters affecting the behavior of aerosol, the mechanisms for generating aerosol, the sources of aerosol and the effects of aerosol on human health and the environment has been presented. It is followed by a discussion on graphite burning in the event of a postulated air ingress accident in a nuclear reactor. The literature review examines the salient findings in this area of study. The gaps in literature that need to be further explored are presented and the justification of the present work in the light of above has been explained.

1.1 Introduction

For all commercial and industrial activities, energy is the lifeblood of our contemporary culture. Fast growth of the global population and economy generates an enormous increase in energy demand. Apart from meeting growing power demands, it is essential to reduce emissions of contaminating gases and combustion products (Chen et al., 2014). According to the World Health Organization, the world's largest environmental threat is pollutants caused by air sources such as energy generation or indoor air pollution (WHO, 2005). Nuclear power plants play a significant role in meeting energy demands and control of pollutant emissions (Yuan et al., 2017). Almost no greenhouse gas or air pollutants are generated during operation and very small emission levels are generated through their entire life cycles (Wang et al., 2019). Nuclear reactors of the type PWR, PHWR, BWR, AGR and Magnox etc. have been in use for decades.

For further enhancement in power production efficiency, HTRs offer a vital alternative. In HTRs, since power is produced at a higher temperature than conventional reactors, the efficiency of this type of reactor is enhanced. However, safety issues also need to be addressed in nuclear reactors (Fallis, 2013). The Chernobyl accident of April 1986 and the recent Fukushima accident of March 2011 have underscored the need for better design with in-built safety mechanisms so that nuclear power gains better acceptance in society. One of the potential risk to the safety of nuclear reactors is air-ingress in case of failure of the containment shield (Adamantiades and Kessides, 2009; Beresford et al., 2019).

In India, the HTR technology development program has been initiated with the aim of providing high-temperature process heat for nuclear hydrogen generation through water splitting (Dulera et al., 2017; Dulera and Sinha, 2008). With the high-efficiency production of hydrogen requiring process heat of around 1123 K, a challenging technology development objective for high-temperature reactors was set to achieve a coolant temperature of 1273 K. The Innovative High Temperature Reactor (IHTR) and the Compact High Temperature Reactor (CHTR) are presently under construction. The current version of the CHTR design consists of uranium-235 TRISO (Tristructural-isotropic) coated particulate fuel, a beryllium oxide (BeO) modulator, a graphite reflector and a lead-bismuth eutectic (LBE) coolant. The design includes many reactor heat removal passive safety systems. Current IHTR designs are based on the configuration of pebble bed fuel with molten salt as coolant (Dulera et al., 2017). The heat of the reactor is passively eliminated by the natural circulation of the coolant for both reactors.

In both prismatic and pebble-bed designs of HTRs, graphite is used as a moderator. Due to factors such as oxidation, abrasion, coolant erosion, quick neutron injury, spalling and flaking, carbonization etc. dust would be generated in the reactor (L. Peng et al., 2016; W. Xu et al., 2017). Large amount of dust in Indian HTR is not expected, since

molten Pb-Bi coolant is substituted for the He coolant. However, in case of failure of coolant pump, leading to a loss of coolant accident (LOCA), the temperature of the nuclear rods may shoot up resulting in melting of the reactor core and air ingress into the system (Englert et al., 2017; Ferng and Chi, 2012; Stanculescu, 2010). High temperature graphite, when exposed to the air would lead to its oxidation, resulting in dust generation. This graphite dust, laden with fissile material from the nuclear rods could be a potential threat because of its ability to travel large distances from the accident site (Chen et al., 2017; Huang et al., 2014; Moormann, 2011).The schematic of this process is shown in Figure 1.1.

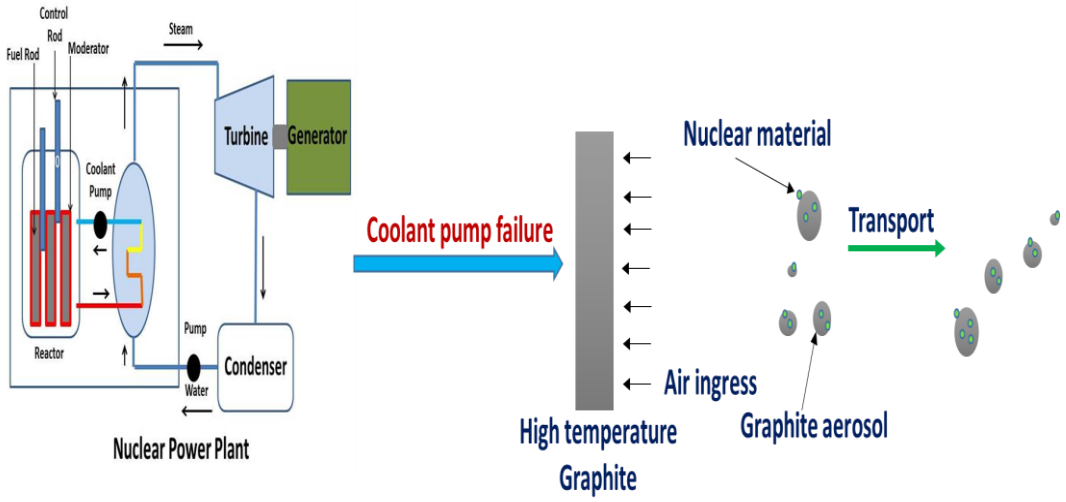

Figure 1.1: Schematic representation of graphite aerosol generation and nuclear material transport during air ingress accident

The graphite particles produced in ultrafine sizes pose an additional inhalation hazard. Due to their small size, these particles have a relatively longer period of residence and increased interfacial activity due to the high surface area per unit mass. Hence it is of utmost importance to gain an understanding about the properties of aerosol generated in an accident scenario.

1.2 Aerosol

The term aerosol refers to the suspension of liquid/solid particles in a gaseous medium. The word aerosol is similar to hydrosols (meaning "water droplets") in the form of a gas phase. Aerosol are two-phase systems consisting of a suspended solid/liquid phase and a gas phase. Aerosol are produced by converting gases into particles or by disintegrating them into finer components through fluids or solids (William C. Hinds, 1999). Aerosol are all-encompassing; airborne soil particles, airborne cloud droplets, power generation smoke, welding fumes, airborne volcanic eruption particles, sea salt sprays, and cigarette smoke particles are all examples of aerosol. Aerosol can be used to describe many commonly recognized phenomena such as dust, fog, smoke, suspended particles, mist, hazelnuts, clouds or smog. Aerosol measurements have increased dramatically in several areas in recent decades, such as air pollution, human health, nanotechnology, atmospherics, pharmaceuticals and medicinal products (Baron, 2011). In the present work, the aerosol consists of solid graphite (carbon) particles suspended in air.

1.2.1 Major parameter affecting aerosol behavior

1.2.1.1 Particle size

Particle size is the most significant parameter for determining the mobility, gravitational settling, diffusion, optical behaviour etc. of aerosol. The particles having different size are governed by distinct physical laws. For example, smaller size particles approximately equal or slightly larger than gas molecules are governed by Brownian motion, while the large particles in micro size range are influenced by the force of gravity and inertia (Von Der Weiden et al., 2009). The particle diameter is an unequivocal and generalized index for the size measurement of particles. A universal characteristic size is

more challenging to identify for non-spherical particles such as fiber and agglomerates. There are several definitions of particle size based on particle properties and particle behaviour and are shown in Figure 1.2. Aerosol science most frequently uses the notion of equivalent diameter to "allocate" a particle size that reflects its specific physical property. The equivalent diameter of a sphere with the same value as the particle to be considered is indicated as the diameter of a certain physical property. For example, the equivalent aerodynamic diameter is the diameter of a standard-density (1000 kg/m^3 or 1 g/cm^3) which has the same terminal velocity, when it settles into gravity as the particle being considered (Baron, 2011).

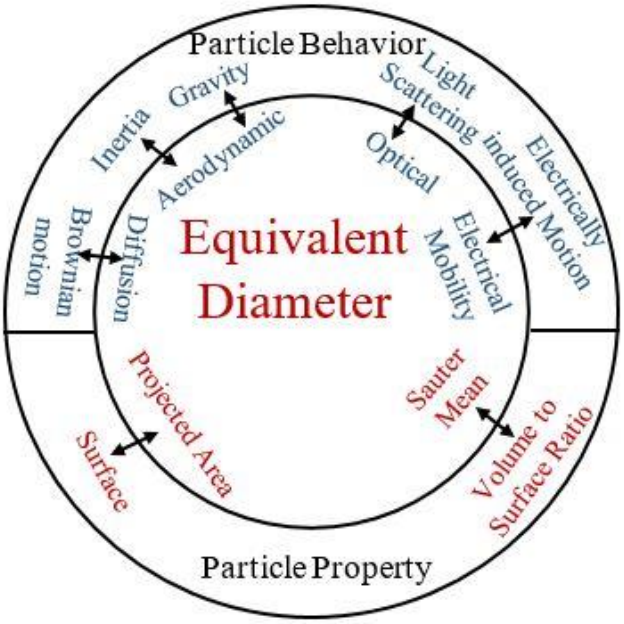

Figure 1.2: Definition of particle size depending on particles properties and behaviour

1.2.1.2 Particle size distribution

The most significant characteristic of polydispersed aerosol is size distribution. Particle size distribution is very essential for understanding the mechanism of aerosol formation, source of generation and its optical behaviour. It was found that particles of a given size are associated with a particular type of phenomenon, depending on mass, size

and nature. For example, coarse particles are responsible for the formation of cloud and ultrafine particles for respiratory problems. Depending on the source and production mechanism, aerosol size varies and extends over wide range. On the basis of size, the aerosol are broadly classified as:

- **Aitken particles**

  Particles radius less than 0.1 μm (nucleation mode);

- **Large particles**

  Particles radius in the range of 0.1 to 1.0 μm (accumulation mode);

- **Giant particles**

  Particles radius larger than 10 μm (coarse mode).

1.2.1.3 Particle concentration

Aerosol concentration is the most commonly measured aerosol property and the most important one for the health and environmental effects. Aerosol concentration are defined in distinct ways, depending on the application. Number, mass, surface area, volume concentration are the most common types of particulate concentration. For example, cleanrooms and atmospheric cloud condensation nuclei are characterized by the concentration of particle numbers. In many particle toxicology research, surface area concentration can be crucial. In some engineering applications where the overall viscosity of the suspension is of interest, volume fractions i.e. volume of particulate matter per unit gas volume is often used as a measure of particulate concentration.

1.2.1.4 Particle forces

The aerosol behaviour also depends upon the cohesive (intra-molecular) and adhesive (inter-molecular) forces which is responsible for holding the particles together and to a surface respectively. These forces are influenced by particle bulk properties of

surrounding gases (temperature, humidity), particle surface parameters (size, shape, roughness, chemistry) and the mechanism of contacting particles (contact time, relative velocity). For example, a particle is moved into the force field when it is subjected to an external force, such as gravity and an electric force. The speed of the migration in the force field is dependent on the particle size.

1.2.2 Effects of aerosol on environment and human health

1.2.2.1 Impact on environment

Aerosol directly affects the radiation balance of the earth by absorbing and dispersing the sunlight. Specific aerosol scatter and absorb sunlight in varying degrees, depending on their physical properties. Because aerosol consist of a wide range of particles with different properties, the overall effect (cool or hot the earth) depends on the amount of light that is dispersed or absorbed. The effect of aerosol on light (i.e. scattered or absorbed light) depends primarily on the composition and color of the particles (Riemer et al., 2019). In general, bright color and translucent particles tend to reflect radiation in all directions and back to space. Pure nitrates and sulfates particles reflect almost all radiation falling on them, cooling the atmosphere. However, dark aerosols can absorb large amounts of light. The black carbon readily absorbs radiation, heats the atmosphere but also shade the earth's surface (Cheng et al., 2009; Hansen et al., 2000; Jacobson, 2000). Long-range transport and deposition of elementary carbon on ice glaciers could be responsible for the melting of glaciers in the Himalayan (Ming et al., 2008) and Arctic regions (McConnell et al., 2007; Ramanathan and Carmichael, 2008). Organic carbon, also referred to as brown carbon or organic matter, has a warming atmospheric effect depending on the brightness of the underlying ground (Arola et al., 2011; Chen and Bond, 2010; Kirchstetter et al., 2004).

Aerosols also play a key role in forming clouds. In the atmosphere, there would be fewer clouds without aerosols. Aerosols act as Cloud Condensation Nuclei (CCN) around which cloud droplets are formed. Aerosol concentration in clouds influences the microphysical, optical properties, precipitating, and lifespan characteristics of clouds (Koch and Del Genio, 2010). Carbonaceous combustion aerosols are important for global concentrations of CCN (Singla et al., 2019; Spracklen et al., 2011) and for changes in cloud properties (Bauer et al., 2010; Jacobson, 2010). The warming effects produced by aerosol (absorbing sun radiation) lead to cloud evaporation(Huang et al., 2019; Toll et al., 2019). This allows more solar radiation to reach the earth's surface.

In addition, aerosol influences the composition of the atmosphere and creates the issue of visibility by dispersing and absorbing light. Without aerosols, our visual range would be about 300 km, limited by the scattering of air molecules. Usually, anthropogenic aerosols in urban environments reduce visibility by one order of magnitude relative to unpolluted conditions. In U.S. national parks such as the Grand Canyon and the Great Smoky Mountains, the loss of exposure from anthropogenic aerosol is a serious problem. Reducing visibility at high relative humidity is more likely to occur as aerosol swell due to water absorption, increasing the cross-sectional region of dispersion, a phenomenon known as haze.

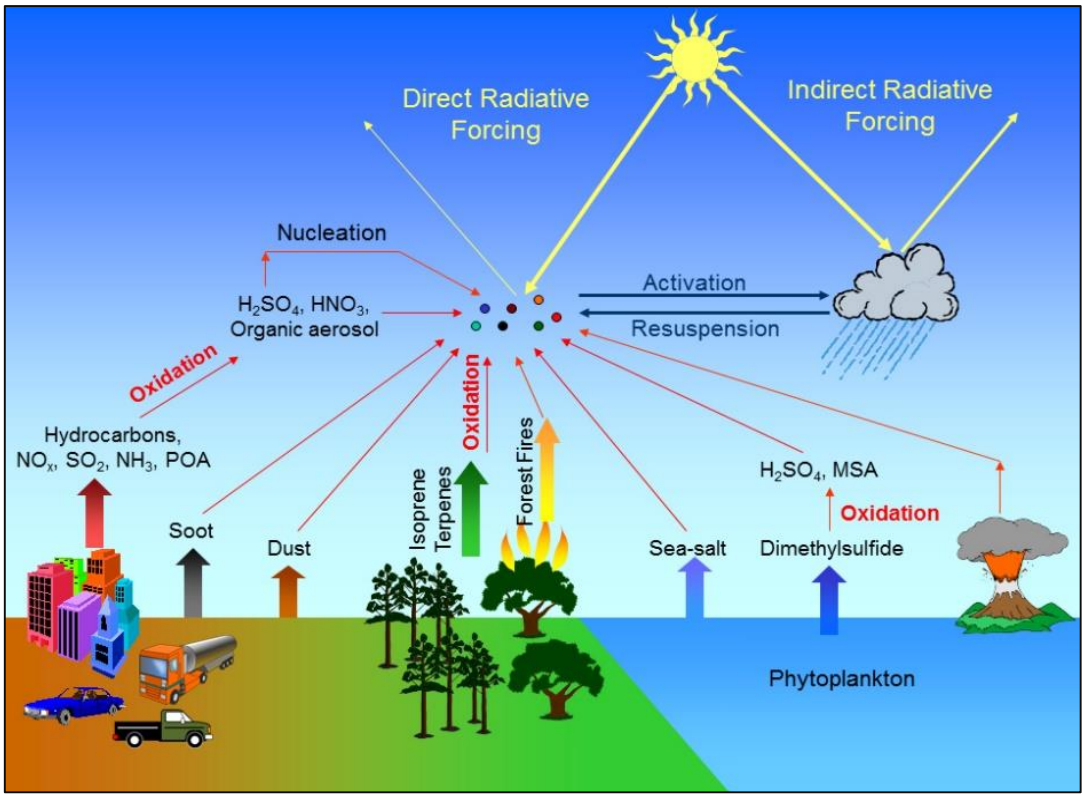

Figure 1.3: Aerosol effects on environment (Kelly, 2016)

1.2.2.2 Impact on human health

In addition to their role in the atmosphere, human health is also affected by aerosols. Inhalation of airborne particulate matter generally leads to premature mortality and morbidity. A fine particulate matter (PM) carries a higher toxic element than coarse PM (Fang et al., 2000). It is highly toxic to humans, due to their bioaccumulation pattern in the biological system (Du et al., 2013). Ingestion, inhalation and dermal absorption are the main routes of intake of these toxic substances (Du et al., 2013; Hu et al., 2012). These fine PM migrate from lung to blood with adsorbed toxic substances (e.g. heavy metals) that cause many diseases (Bond et al., 2013). It increases breathlessness, wheezing and asthma, cough, lung cancer, chronic obstructive pulmonary diseases (Jiang et al., 2016; Mukherjee et al., 2014). It may also cause skin effects, hematopoietic and nervous systems which interfere with the heart (Zhang et al., 2014). Indoor aerosol induced

syndromes, infections, and sensitivities. A toxic element such as Pb and Cd may be carcinogens to humans. In addition to the carcinogenic effect, Pb induces neuropathy, renal impairment and encephalopathy, and Cd also interferes with normal kidney function (Jaishankar et al., 2014). Cr causes lung cancer, skin disease (Proctor et al., 2014) and teratogenic effects and human carcinogenic effects (Cr(VI)) (Dayan and Paine, 2001).

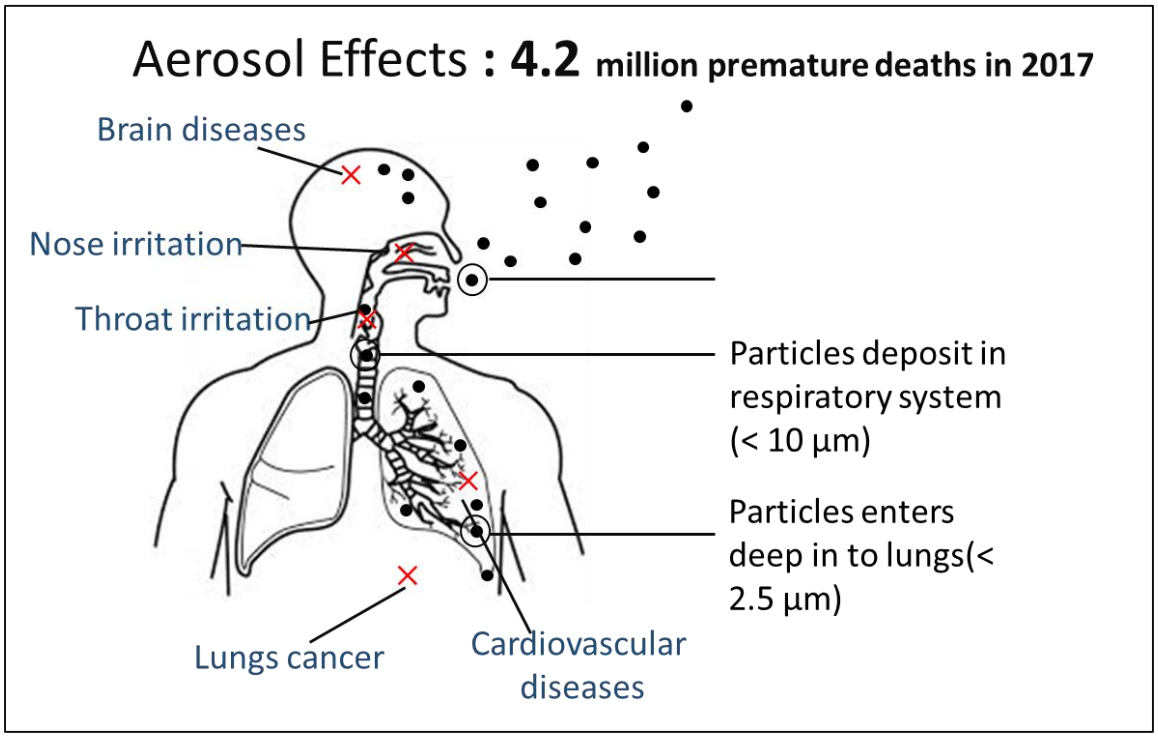

Figure 1.4: Effects of aerosol on human health

1.2.3 Sources of aerosol

In estimating the consequences on climate and health by airborne particulate matter, awareness of sources and emission of aerosols are essential. There are different sources of aerosols and these sources can also vary with time. The aerosol sources can be both natural and anthropogenic (man-made). Natural or primary sources include soil-generated dirt from winds, sea spray and volcanic activities etc., while industrial emissions, biomass

burning and vehicular emissions etc. come under the category of anthropogenic or secondary sources.

1.2.4 Mechanism of aerosol formation

As we have discussed in the previous section, aerosols from both natural and anthropogenic sources directly affect the Earth's radiative balance by scattering and absorbing light, and they also indirectly impact radiative transfer by altering cloud formation and cloud properties. So, it is very essential to understand the mechanism of aerosol formation in order to reduce the effect of aerosol on the environment and human health. Most of the aerosol are formed by the following mechanism:

- Mechanical disintegration process (primary sources)
- Process of gas-to-particle conversion (secondary sources)

1.2.4.1 Mechanical disintegration

The fine sand and soil particles transmitted by wind become an airborne particle. The presence of irregular soil and sand particles in a rough terrain causes turbulent air movements, which collect the particles from the surface and deposit it into the atmosphere. The ocean waves, which generate scrap droplets at the crests in strong wind conditions, are another form of mechanical production of aerosols. There are different kinds of organic particles like pollens, seeds, spores and leaf fragments, produced by crops, dispersed by atmospheric circulation form different types of primary source of aerosol, especially in forest and dense vegetation regions.

1.2.4.2 Gas-to-particle conversion

The nucleation/condensation of low volatile gasses mainly generated by industrial activity, biomass burning, forest fires, etc., produce the particles. This mechanism of

formation of aerosol is called gas-to-particle conversion. There are two types of nucleation processes for gas-to-particle conversion: homogenous and heterogeneous nucleation. The precursor gases directly condense to form a new particle in homogenous nucleation process. Homogeneous nucleation-produced aerosols cover a wide range of size, but mostly in the range of nucleation mode particles (< 0.1 μm). In heterogeneous nucleation process the precursor gases condense on the surface of other pre-existing nuclei to form particles.

1.2.5 Measurement of aerosol

Aerosol measurements are carried out by environmental engineers and industrial hygienists in order to measure the level of concentration of harmful aerosols which can affect the environment and human, while atmospheric scientists measure aerosols to understand their impact on the world climate. Aerosol measurement protocol is more complicated, time consuming and requires a lot of resources. Therefore, developing a cost-effective instrument for measuring aerosol properties requires a better understanding of aerosol behaviour.

Most of the techniques for the measurement of aerosol properties are based on two categories: first one is the collection and subsequent testing of aerosol particles on a substrate, for example a filter and the other one, a real-time, in-situ measurement. The collection followed by measurement has traditionally been used extensively as a means of utilizing many powerful laboratory analysis methods (inertial, gravitational, centrifugal, chemical analysis, X-ray analysis etc.). This strategy has however a limitation because particles can be altered through transport and collection procedures, the readings are time averaged and not instantly accessible. On the other hand, in-situ measurements can give the results at every instant of time. Due to limit of the measurement device during in-situ measurements, particles can have less characterization i.e. concentration limits,

size distribution limits etc. Therefore, based on the application a variety of technique and devices can be used for aerosol measurement. Particle measurement methods and instruments are shown in Figure 1.5. The most important properties of aerosol are particle concentration and size. The concentration of particles can be measured in mass (m), number (N) and surface area (S) using different measurement principles such as gravimetric, optical, microbalance and electrical charge. In gravimetric method, the concentration of the particle mass is determined by weighing the filters before and after the sampling period. Optical devices measure the particle concentration by detecting the light scattering from particles that are taken into a device (e.g., optical particle counters) and optical systems that detect particles directly outside the device without extracting samples (e.g., forward scattering spectrometer probes). Optical methods that use visible light wavelengths (from 400 to 700 nm) cannot investigate particles smaller than the wavelength of visible light. An aethalometer is a soot detector, which is dependent on the absorption of light in filter samples to determine the concentration of black carbon (BC) in ambient air. In the microbalance method, the particles are collected over the surface of the oscillatory microbalance element, using the alteration of the resonance frequency to determine the PM (particulate matter). Sampling of aerosol for analysis of particle size in a microscope generally involves collecting particles directly from filters followed by filter preparation to improve visibility. In addition to the dimensions of solid particles, electronic microscopy also examines their morphology. Differential mobility analysers (DMA) classify particles according to their electrical mobility, which depends on particle charge, gas properties and the geometric particle size, and then particles size and concentration are measured using an electrometer or CPC. The CPC measures the total aerosol number concentration larger than some minimum detectable size. It works by

growing particles by condensation in a supersaturated environment until they are sufficiently large to be detected optically.

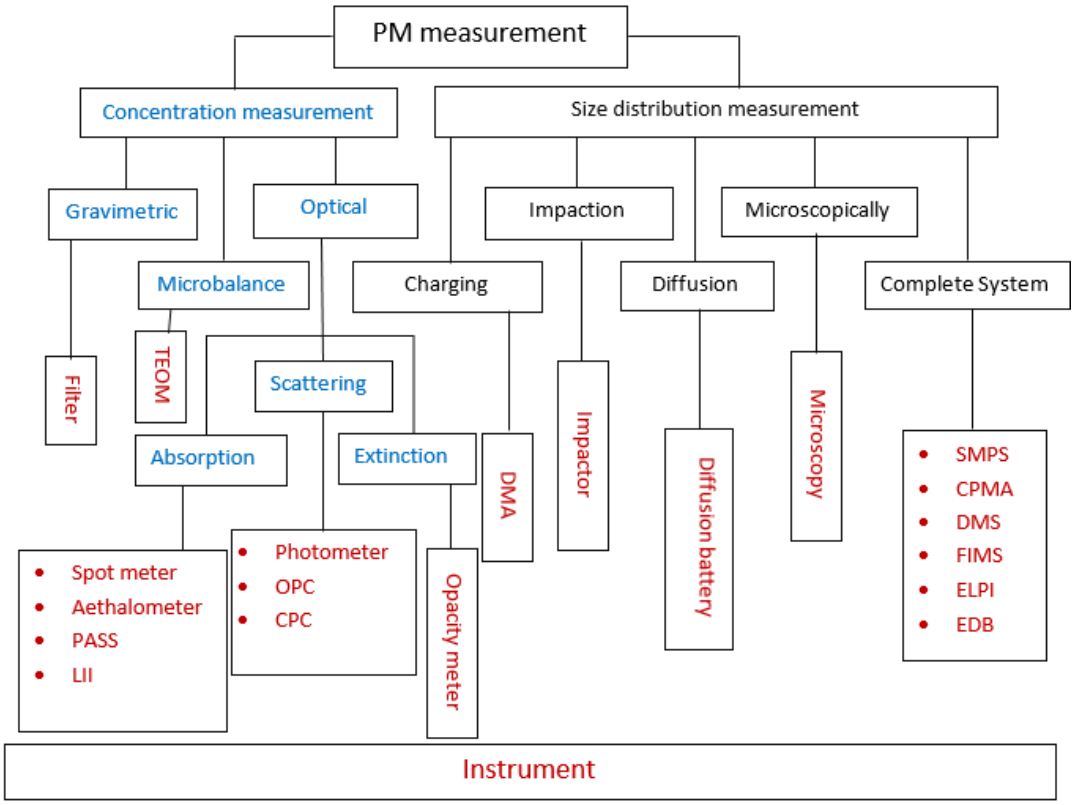

Figure 1.5: Method and instrument of particles measurement

However, measuring high temperature aerosol in a closed combustion setup, as is the case in the present work, presents new challenges and problems (Deuerling et al., 2010). Due to the presence of a combination of gases and particles generated at high temperatures, it is difficult to analyse the combustion products (Glytsos et al., 2010; Tiwari et al., 2014). The maximum sample temperature limit of many aerosol spectrometers commercially available for handling is less than the temperature at which aerosol are sampled, and hence aerosol must be cooled prior to spectrometry. The high temperatures involved can give thermal shocks to the components in the setup. To maintain structural integrity of the heated components, appropriate cooling arrangements must be integrated into the experimental setup. Due to a decrease in temperature, the

nucleation and condensation procedures are anticipated to change the particle properties (Thanh et al., 2014). Consequently, the correct aerosol size distribution at elevated temperatures is difficult to measure. The sealing of the closed combustion system for restricting air transfer from or to the system also becomes a difficult task at high temperature.

1.3 Graphite

Graphite is a crystallized form of a carbon element and has a hexagonal structure (Figure 1.6). Graphite occurs naturally and under ordinary conditions, is the most stable form of carbon. It is found in meteorites, metamorphic rocks, igneous rocks. It can be transformed into a diamond at elevated pressures and temperatures. It is very useful for electrical products such as electrodes, batteries, solar panels and its outstanding moderator characteristics make it beneficial for nuclear reactors.

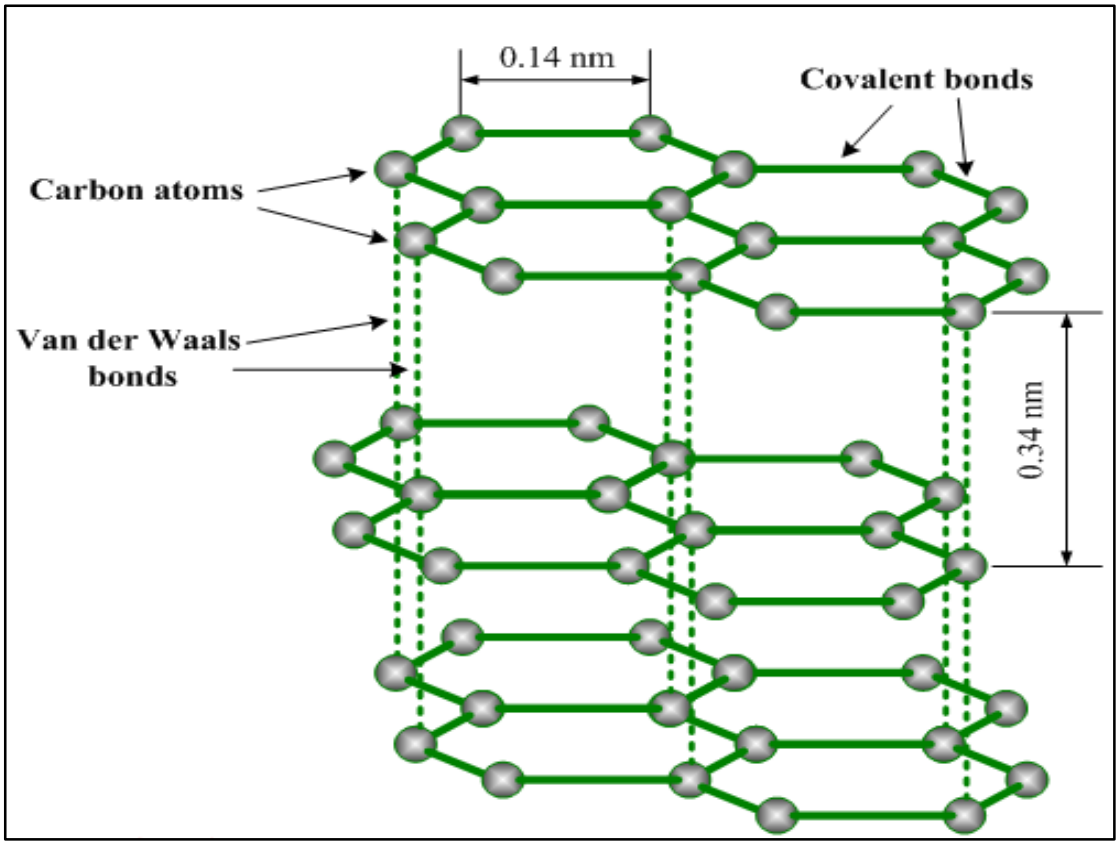

Figure 1.6: Structure of graphite

1.3.1 Physical properties

- **Physical state**

The graphite has color from steel gray to black and is odorless. It is opaque and its luster is sub-metallic. It has a smooth, greasy texture and can be readily broken. Although graphite is flexible and smooth, it is not elastic.

- **Structure**

Graphite is crystalline in nature, but perfect graphite crystals are rarely found. Graphite carbon atoms are hexagonally arranged in a plane forming a condensed ring system in their composition. This gives a hexagonal shape to the graphite crystals. Each graphite layer is joined by a weak covalent bond to form a giant covalent structure (Figure 1.6).

- **Melting Point**

Graphite has a high melting point approximately 3000 °C. It is thus suitable for a wide range of temperatures applications.

- **Density**

As the graphite plane are held by a weak covalent bond with a large amount of vacant space, the density of graphite varies from 1.80 to 2.33 g/cm^3.

- **Solubility**

Graphite is insoluble in water and other organic solvent. The structure of solvent molecules and carbon atoms does not have attractive forces and therefore it does not dissolve in any of this organics solvent.

- **Thermal conductivity**

In the carbon layers of graphite there is a large number of free electrons. Free electrons can move freely and conduct heat, making graphite a good heat conductor.

1.3.2 Chemical properties

The chemical reactivity of graphite is exceptionally low which explains its geochemical stability, demonstrated by the existence of natural ores in the earth's crust. To convert graphite into the thermodynamically-favored carbon dioxide, it needs extremely powerful oxidants. This also allows the use of graphite in nuclear reactors and industrial applications.

1.3.3 Background of use of graphite in nuclear technology

In the past it was found that the nuclear fission of radioactive materials like uranium, plutonium, thorium etc. could be utilize for power generation. The fission of radioactive materials produces an uncontrolled chain reaction that was first discovered by Otto Hahn and Fritz Strassman in 1939. In order to properly control the nuclear chain reaction, it is very important to slow down the fission of neutrons before other atoms are caught in the nuclear chain reaction of the radioactive material. It became known by the end of 1939 that the two most promising moderators, heavy water and graphite, could be used to slow down the speed of neutrons. Heavy water is a good moderator, but it also has a high tendency to absorb neutrons due to the presence of hydrogen atoms in water.

Graphite has a low tendency to absorb neutrons compared to heavy water. Keeping this in mind, the first Chicago Pile-1 artificial nuclear reactor was built in 1942 (Fermi, 1952). It was the foundation for future innovations in the various graphite-moderated nuclear reactors. AGOT graphite was used for the building of the X-10 graphite reactor at Oak Ridge TN (early 1943) and the first reactors at the Hanford plant in Washington (mid-1943) (IAEA, 2001). The first graphite reactor in France was the EL2 built at Saclay

in 1952. It was an experimental reactor like the EL3 built in 1957. The total mass of graphite in these two reactor was 109 tons (Fachinger, 2012). High-temperature gas-cooled reactors (HTGRs) were developed in the early 1960s throughout the United Kingdom, the United States and Germany. In 1991, Japan began the construction of a 30 MW High Temperature Test (HTTR) reactor, which reached its first criticality in 1998. In China, a 10 MW experimental high temperature gas-cooled reactor (HTR-10), whose design started in 1992 and construction commenced in 1995, reached it criticality in the end of 2000 (Wu et al., 2002). Later others countries like India, Russia, France etc. started the development of high temperature nuclear reactor in which large amounts of graphite are required.

1.3.4 Review of studies on graphite oxidation during air ingress in a nuclear reactor

Several studies on the issue of burn-initiation in nuclear systems were carried out after the fire at the Windscale Reactor (Fachinger, 2012; IAEA, 2001; Rush et al., 1977). Schweitzer et al. conducted the most thorough and successful experiments at BNL (Brookhaven National Laboratory) (Schweitzer, 1962). These studies have been conducted primarily to comprehend the possible combustion of the graphite moderated and air-cooled BNL reactor in 1960s. Graphite channels were heated to a certain temperature in a furnace. When a stable temperature profile was reached, the airflow at initial temperatures between 300 °C and 350 °C entered the internal hole of the channel and the temperature development inside the channel was recorded. The findings of the studies highlight that graphite burning depends primarily on the graphite reactivity, the thermal equilibrium depending on the geometry of graphite, flow rates etc.

Research related to transport of graphite dust has been primarily carried out in 1. JAERI (Japan Atomic Energy Research Institute) by Hishida and Takeda, 1991 and 2. NACOK (Naturugim Core mit Korrosion) in Julich Research Centre, Germany (Zheng

and Stempniewicz, 2012). The research focused on gaining a deeper insight into the basic phenomenon of diffusion, natural convection and chemical reactions that are supposed to take place in the event of air ingress. Experimental facilities were established to study these phenomena in three stages comprising of-

1. Depressurization that results when there is a breach in the coolant circuit and air ingress occurs.

2. Study of helium-air interaction which is a molecular diffusion driven phenomenon and takes place over a few hours of time span.

3. With passage of time, buoyancy driven effects come into play due to the temperature gradients existing in the system. Due to natural convection effect, air enters the inner tube of the primary pipe, passes through the high temperature passage and exits from the outer tube of the inner pipe.

The generation of graphite dust in the reactor, its interaction with the FP (Fusion product) and the subsequent transportation and deposition of the FP laden aerosol within the primary circuit and outside it (within the reactor building) was characterized by study of graphite component degradation and interaction with FP and thermal fluid transport respectively.

Experimental facilities for graphite dust related thermal hydraulics studies have also been set up or being designed at the THAI (Thermal-hydraulics, Hydrogen, Aerosol, Iodine) project in Frankfurt, Germany as well as Paul Scherrer Institute in Switzerland (Gupta et al., 2010).

In the proposed THAI experiments, a rigid multi-compartment container of volume 60 m^3 (~ 9 m in height 3 m in diameter) is to be supplied with He-graphite dust from an external tank. Sensors would detect the relevant process parameters. Instrumentation

includes 2D/3D PIV velocimetry and laser Doppler anemometry for flow measurement, heat conductivity sensors for gas concentration measurement etc. The measured values would be used as an input in validating the CFD simulation of the phenomena.

Besides experimental work, simulations using CFD tools have also been carried out to address the issued related to air ingress in HTGR. CFD analysis using a commercially available software FLUENT have been carried out by Kadak and Zhai, 2006. Other dedicated software includes MELCOR which is a fully integrated engineering software developed at Sandia National Laboratories for U.S. Regulatory Commission. The SPECTRA code is an accident analysis code developed in Netherlands. ECART is an integral systems code which was initially designed for Light Water Reactors and can treat a wide range of aerosol phenomenon. Fortunately, ECART can be freely downloaded from the internet. The current NGNP (Next Generation Nuclear Plant) Project of the U.S. Department of Energy is employing MELCHOR code for study of HTGR. SPECTRA code will be used for code comparison (The U.S. Department of energy, 2010).

1.3.5 Graphite oxidation

Nuclear grade graphite has a number of desirable characteristics, such as excellent moderation capacity with low neutron absorption, appropriate heat resistance, high thermal, conductivity, chemical stability, low expansion coefficient etc. (Park, 2018; Zhou et al., 2018). As we seen from above section, a large quantity of graphite is used in a nuclear reactor. For environmental safety and long term operation of nuclear reactors, it is very essential to understand the combustion behavior or chemical kinetics of graphite.

1.3.5.1 Chemical kinetics

Rapid chemical reaction of two or more substances with a characteristic liberation of heat & light is called combustion. There are two types of combustion: homogeneous-

where equal amounts of substances are mixed and heterogeneous- where unequal amount of substance are mixed. Burning of carbonaceous materials was probably the first chemical reaction, which mankind learned to handle (as wood and charcoal fires for heating and cooking), but a complete theory of burning was not developed earlier than about 1930s, which is later than, for example, quantum theory. Main contributions to a theory of burning phenomena came from the Russian scientists, Frank-Kamenetzkii and Semenov (Moormann, 2011). The progress of burning may be dominated by thermal effects, as is the case in burning of solids or - as often found in gases- may propagate by chain branching. The thermal ignition of graphite depends on the activation energy, internal temperature rise, simple kinetics, ambient environment.

The most important chemical reactions occur during air ingress into the HTR core with graphite burning are listed in Table 1.1, together with their reaction enthalpies, ΔHR. Whereas the heterogeneous primary burning reactions (1a) and (1b) and the homogeneous CO burning reaction (3) are exothermic, the boundary reaction (2) proceeds endothermically. It should be noted that graphite oxidation belongs to reactions with solely gaseous products, which proceeds to some extent different from reactions with solid products. Lack of success to burn large graphite blocks even led to the opinion that high-purity nuclear graphite cannot burn (Theodosiou et al., 2017).

Table 1.1: Chemical reactions relevant in graphite burning

Sl.No.	Reaction	ΔH_g (kJ/mol)	Type
1a	$2C + O_2 \rightarrow 2CO$	−221.04	Heterogeneous Primary
1b	$C + O_2 \rightarrow CO_2$	−393.51	Heterogeneous Primary
2	$C + CO_2 \longleftrightarrow 2CO$	+172.47	Boundary reaction
3	$2CO + O_2 \rightarrow 2CO_2$	−565.98	Homogeneous

1.3.6 Solid - Fluid reaction

This section deals with the class of heterogeneous reactions where a fluid contacts with a solid, reacts with it and turns it into a product. Such responses can be depicted by

$$\text{A (solid)} + \text{B (fluid)} \rightarrow \text{Solid and fluid Products}$$

When solid fuel reacts, two conditions arises: (a) when the particles involved in the reaction do not shrink as the reaction progresses, (b) the particle shrinks as the reaction progresses. Based on these conditions, there are two idealized models for the non-catalytic reaction of the particles to the surrounding fluids:

- Progressive model
- Shrinking core model

1.3.6.1 Progressive model

In the progressive model, the reactive gas enters and reacts at all times throughout the particle, most likely at different rates at different locations within the particle. Thus, the solid reagent is continuously and progressively converted throughout the particle as shown in Figure 1.7.

When solid fuel burns at a low temperature, the combustion products generated during burning are much lower, resulting in a small thickness of the combustion layer generated on the solid fuel. In this domain, oxygen first diffuses into the film and then reacts with the core of the sample. The thickness of the film is very small, so oxygen can easily penetrate into a sample and reacts throughout the sample with distinct rates at different locations (Remiarova et al., 2004; Zajdlik et al., 2001).

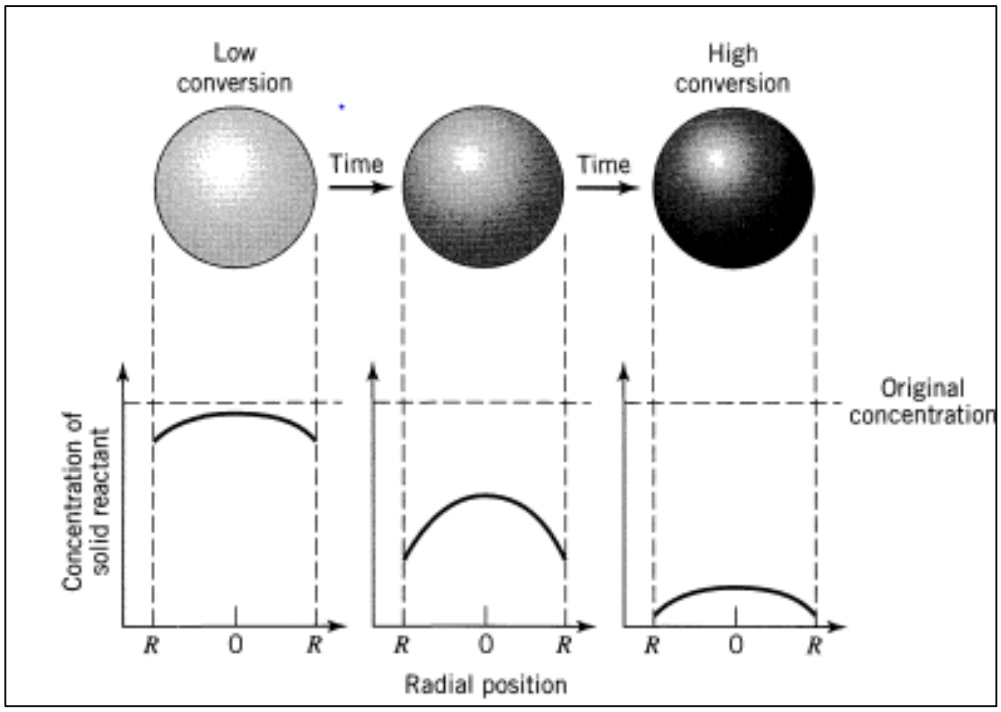

Figure 1.7: Progressive model (Levenspiel, 1964)

1.3.6.2 Shrinking core model

The shrinking core model was first reported by Yagi and Kunii, 1961, and was explained by Levenspiel, 1964. In this model, reactions first start at the outer surface of the particle. The reaction zone then moves inside the reacting core surface leaving behind combustion products. In this model, the core of the particle shrinks in size with time during the reaction (Levenspiel, 1964). The reaction proceeds in five steps (Figure 1.8):

- Diffusion of gases reactant through the film surrounding the particle to the surface of solid.
- Penetration and diffusion of the gases reactant through the solid products layer.
- Reaction of the gases reactant with solid fuel at the core surface.
- Diffusion of gaseous products through the ash layer back through the exterior surface of the solid.
- Diffusion of gaseous products through the gas film back in the fluid main body.

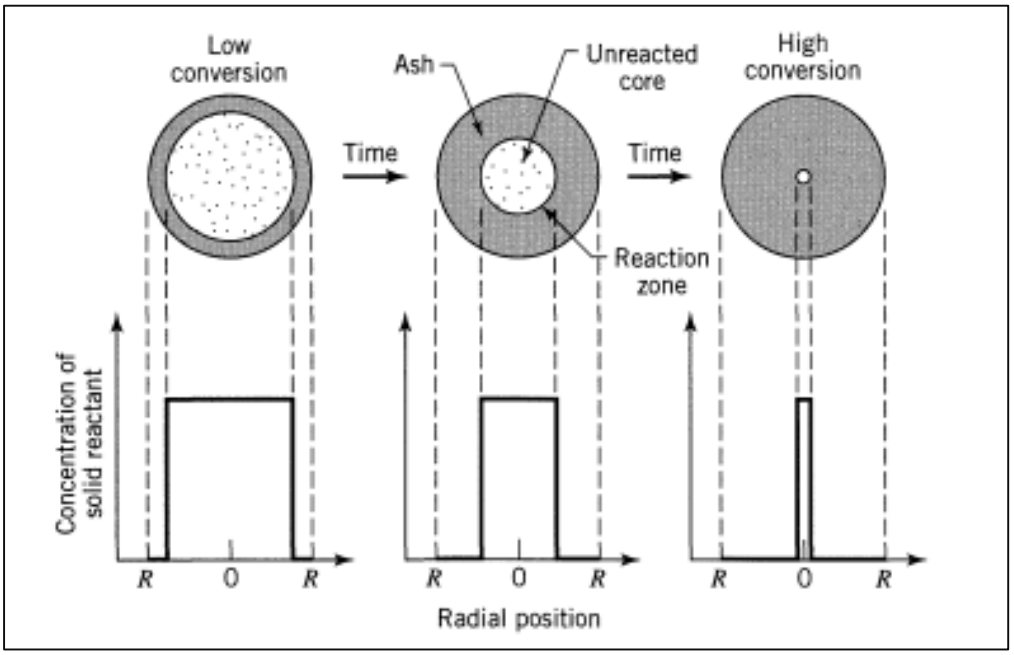

Figure 1.8: Shrinking core model (Levenspiel, 1964)

1.3.7 Literature survey on oxidation of graphite

In the past, some authors studied the impact of the role of graphite oxidation under postulated nuclear accident conditions. They hypothesized the effect of materials and environmental factors on oxidation reaction in nuclear systems (Kane et al., 2017a; Liu et al., 2015; Loren Fuller and Okoh, 1997). Propp, 1998, there were three regimes for graphite oxidation: the chemical regime, the controlled boundary layer regime and the controlled in-pore diffusion regime (Figure 1.9). Chemical regime occurs at lower temperature, in which the reaction occurs between graphite and oxidizing gas is very slow. The oxidation rate depends on the intrinsic reactivity (material microstructure) and concentration of gas phase oxygen. So, the rate of oxidation is slowly controlled by chemical reactivity of graphite. In this regime, oxygen penetrates deep into the graphite. The material oxidizes homogeneously due to the chemical reaction via its pore system under the rate-limiting step. The boundary layer controlled regime occurs at higher

temperature, the rate of reaction is so fast that all the oxidizing gasses (oxygen) react at the surface of graphite. This reaction remains restricted to the outer surface only so it changes the graphite geometry without damaging the interior material. The concentration of oxidizing gases on the graphite surface differs significantly. The external mass transfer of gas species (O_2, CO, CO_2) to the outer surface is the difussion limited step. The pore diffusion controlled regime lies between the chemical regime and boundary layer controlled regime. The oxidation rate of graphite is controlled by chemical kinetic and oxygen diffusion rate in this regime.

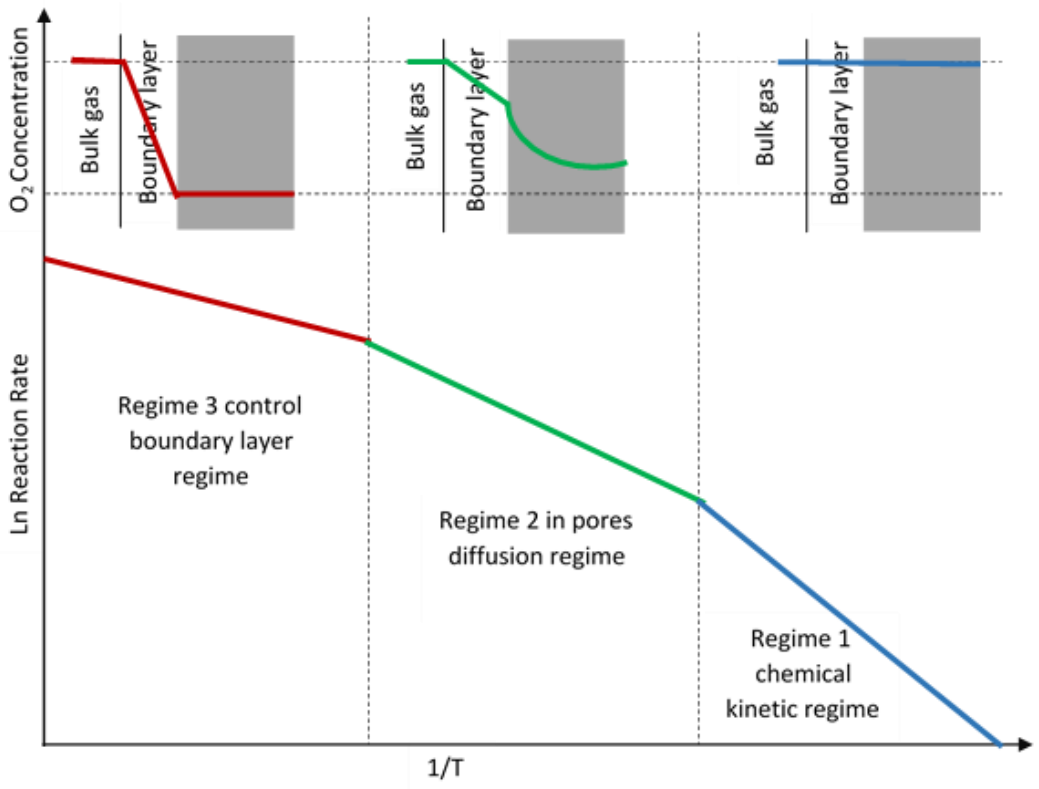

Figure 1.9: Oxidation regimes in graphite

Hinssen et al., 1983, gave the temperature limits of each regimes. Oxidation belongs to the chemical regime at temperatures below 500 °C; oxidation belongs to the in-pore diffusion regime between 500 °C to 900 °C; oxidation belongs to the boundary layer regime at temperatures above 900 °C. Blanchard (Blanchard, 2003) gave another classification that the range of the in-pore diffusion-controlled regime lies between 600

°C to 900 °C. They pointed out that the impurity concentration, density and graphite microstructure influenced the transition temperature. In addition, the size of the specimen is influences the transition temperature.

Contescu et al., 2008, characterized the kinetic parameter for graphite oxidation. They used a standard size (and shape) specimens, large enough in size to accommodate the inherent local microstructure differences between graphite samples. It was found that the transition regime 1 and 2 of graphite depends upon the oxidation temperature and rate of oxygen supply.

Xiaowei et al., 2004, investigates the oxidation behavior of IG-11 graphite by thermo-gravimetric analysis at a temperature range of 400 - 1200 °C. The results of the experiment show that oxidation occurs in three regimes. At a lower temperature range of 400 - 600 °C, the oxidation was controlled by a chemical regime with an activation energy of 158.56 kJ. At an intermediate temperature of 600 - 800 °C, the activation energy was 72.01 kJ/mol. and oxidation is the control by in pore diffusion regime. At higher temperatures above 800 °C, the activation energy is very low and oxidation was controlled by the boundary layer regime. From the above review, we conclude that there are three regimes for reaction in graphite which depends on the temperature range which varies for different grades and impurities present in graphite.

Kane et al., 2017a, provides a brief review of the reaction of graphite with molecular oxygen in terms of energy and mass transport, chemical kinetics and structural evolution. To accurately predict the effects of oxidation on nuclear grade graphite, a new model based on the reaction mechanism, the effects of mass transfer and the graphite pore structure was suggested. The model uses a standardized inherent oxidation rate for the reactive surface area to be used for all nuclear-grade graphite.

Contescu et al., 2012, used thermogravimetric analysis to compare the three grades of nuclear graphite with distinct structures. Based on the grain size, filler shape, and textural characteristics, they recognized found that at low temperature chemisorption is not reliable method for determining the surface of reactive sites during air oxidation.

Chi and Chan Kim, 2017, examined the effects of the air flow rate on nuclear grade graphite oxidation (NBG-18, NBG-25) at a temperature range of 600 - 1100 °C. The effects of flow rates on graphite oxidation were negligible at a lower temperature whereas the effects of the flow rate were significant at higher temperatures (above 800 °C). The overall oxidation rate and flow rate behavior of NBG-18 was higher than NBG-25 at 600 - 800 °C.

Huang et al., 2014, studied two grades of nuclear graphite (IG-110, IG-430) in the temperature ranges of 700 - 1000 °C and found that graphite pores were growing at temperatures above 700 °C. Their experimental results indicate that neither IG-110 nor IG-430 could maintain structural integrity in the range of 900 - 1000 °C during an air ingress accident for more than 1 hour. Their results indicate that at medium temperatures (< 800 °C), IG-430 showed a significant improvement over IG-110. However, as temperature increases, the advantage of IG-430 started to decrease.

Kugeler et al., 1992, studied the aerosol formation due to air and water/steam corrosion on a graphite pebble bed. The experiments simulated hypothetical accidents in high temperature reactors. The particle mass concentration and size distribution were obtained for a wide range of temperatures and different corrosion conditions. At a low temperature of around 650 °C, the particle mass concentration was low and insignificantly affected by air velocity, while at higher temperatures the effect of air velocity became significant. The progress of corrosion also affected the particle size distribution, particle

and mass concentration generated. In both cases (stream and air) the particle size distribution shifted to larger diameters with proceeding corrosion (Kugeler et al., 1992).

When the temperature of graphite exceeds 500 °C, graphite easily reacts with oxygen and burns (Kane et al., 2017b; Makino et al., 1996). To protect graphite from oxidation at high temperatures, different type of ceramic coatings such as Al_2O_3, SiC, $MoSi_2$, ZrB_2, SiO_2, Si_3N_4, B_4C, etc. has been explored to efficiently cut diffusion channel for oxygen to attack the substrate (Feng et al., 2016; Li et al., 2016; Masoudifar et al., 2016; Nechepurenko and Samuni, 2000; W. Peng et al., 2016; Wang et al., 2016; Yang et al., 2014; Zhang and Lee, 2003). Out of these coating options, $MoSi_2$ and B_4C coatings are expected to severely affect the neutronic behavior of the reactor. However, due to limited volume fraction, other coating options are not suspected to modify the neutronic behavior of the core significantly. Alumina has been widely used in nuclear industry as fuel clad and other structural material. Al_2O_3 coating seems to be one of the most promising option for the protection of graphite components due to its strength retention, high melting temperature and superior oxidation resistance. Al_2O_3 coated graphite has lower porosity, higher strength and stability than uncoated graphite(Bahlawane, 2001; Wang et al., 2014; X. Xu et al., 2017; Zhang and Lee, 2003). However, maintaining the purity of coating is crucial as the impurities may adversely affect the neutronic behavior of the reactor. Also, the effect of neutron irradiation on thermal diffusivity could be detrimental for large volume fraction of coating.

1.4 Motivation for the work

As per the available literature, the emphasis in the past has been mostly directed towards studying oxidation effects on graphite. A very few literatures are available on the aerosol generation and its characterization during burning at different conditions. It is very essential to study the behaviour of graphite burning at high temperature and

characterization of the aerosol generated for a bare and a coated sample of nuclear grade graphite for the subsequent use of this knowledge in designing safer reactors. It is expected that the results obtained would be helpful in obtaining valuable information about the measures that may be incorporated for enhanced performance and safety of Indian HTR design. Based on above literature survey, the problem of work has been described and objective of thesis is defined.

1.5 Problem definition

Few questions that arise during graphite burning are:

- What is the effect of temperature and air flow rate on graphite aerosol generation?
- What is the size and size distribution of graphite aerosol generated at different heating conditions?
- Can coatings be used to decrease aerosol generation during graphite burning?
- What is the behaviour of aerosol generation in the presence of coating and how does it compare with the case of uncoated graphite?

1.6 Objective of the thesis

- Development of high temperature facility for graphite burning.
- Study of aerosol generation and its characterization at different heating conditions during burning of (a) Bare Graphite (b) Alumina Coated Graphite.

1.7 Work plan

It is very important to make a work plan for conducting an experiment after the problem has been identified and the objective has been decided. For the present work, first, the experimental setup was designed and fabricated. After the design of the experimental setup, testing of this facility was done. A graphite sample was then prepared

and SEM, TGA, EDS and XRD were used to characterize it. Nuclear grade graphite with and without alumina coating was tested in this facility. In addition to measuring the number and mass distribution of the produced particles at different temperatures and flows, CO and CO_2 emissions have also been monitored. After the completion of each experiment, the residual samples were removed for further analyses. The block diagram of work plan is shown in Figure 1.10.

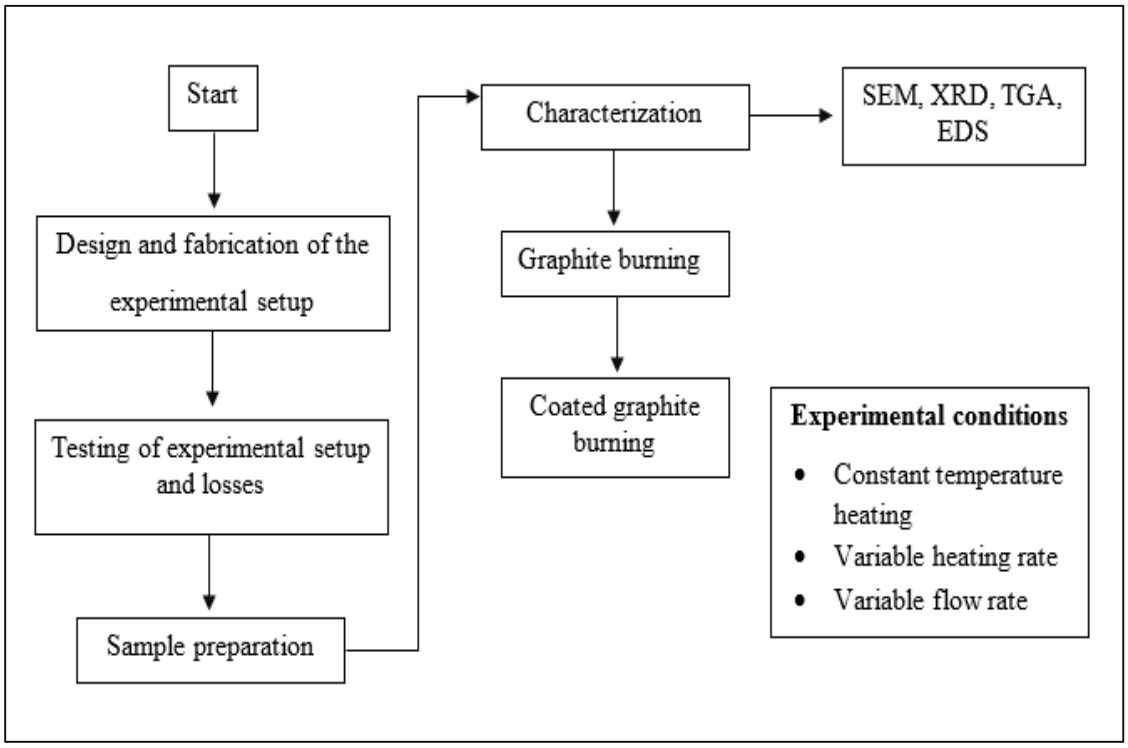

Figure1.10: Block diagram of work plan

1.8 Thesis outline

This work aims to measure and interpret the number and size distribution characteristics of aerosol produce by exposing bare and alumina coated graphite samples to high temperature conditions. An experimental facility is developed and employed for measuring the aerosol characteristics at extreme temperature and concentration conditions. Apart from measuring number concentration and size distributions of

generated particles at different temperatures and flows, emission of CO and CO_2 was also monitored.

This thesis is divided into six chapters. The present chapter contains the background, literature review and motivation for the thesis and outline the objective of the research.

Chapter 2, **Description of the Experimental Set-Up** deals with the design and fabrication of the experimental set-up that was employed to burn the graphite samples and characterize the aerosol produced. Details of the experimental setup components are described in this chapter.

Chapter 3, **Testing of the Experimental Set-Up**, describes the variation of temperature of air with different air flow and heating conditions in the experimental setup. In addition, losses due to diffusion, gravitational, thermophoresis and condensation were also calculated by using empirical correlations.

Chapter 4, **Material Characterization and Experimental Methodology**, provides information about the properties of bare and alumina coated graphite samples. the experimental conditions and procedure followed in this work have also been explained in this chapter

Chapter 5, **Characteristics of Aerosol Generated by Burning of Bare and Alumina Coated Graphite,** reports the graphite and alumina coated graphite particle generation at high temperature conditions and its characterization, especially in terms of number concentration and mean size. The study also relates the emission of CO and CO_2 gases with particles in order to estimate the transition temperature for the generation of graphite particles under the different heating conditions.

Chapter 6, **Conclusion and Scope for Future Work**, summarizes the key finding of the present research work and suggested areas where future work may be carried out.

Summary

As evident from the above information, the problem of air ingress in a HTGR leading to graphite particle generation has been experimentally studied. The experimental work was mainly focused on the design of a suitable furnace for burning the graphite at higher temperature. In addition to this furnace, there should be an assembly attached and integrated with this furnace to ensure supply of clean air and exhaust of aerosol laden air stream. The aerosol generated were characterized for their size, concentration and size distribution using aerosol spectrometers. Regarding the selection of aerosol spectrometer, it was assumed that since black carbon aerosol over a wide size range could be generated during the burning of graphite, no single instrument would be capable of measuring the aerosol produced. After literature survey, it was decided to use a combination of two instruments an SMPS (scanning mobility particle sizer) and an OPS (optical particle sizer) for measuring small and larger particles respectively. The details of the experimental setup are given in next chapter 2.

References

Adamantiades, A., Kessides, I., 2009. Nuclear power for sustainable development: Current status and future prospects. Energy Policy 37, 5149–5166. https://doi.org/10.1016/j.enpol.2009.07.052

Arola, A., Schuster, G., Myhre, G., Kazadzis, S., Dey, S., Tripathi, S.N., 2011. Inferring absorbing organic carbon content from aeronet data. Atmos. Chem. Phys. 11, 215–225. https://doi.org/10.5194/acp-11-215-2011

Bahlawane, N., 2001. Novel sol-gel process depositing α-Al_2O_3 for the improvement of graphite oxidation-resistance. Thin Solid Films 396, 126–130. https://doi.org/10.1016/S0040-6090(01)01259-7

Baron, P.A., 2011. Aerosol measurement principles, techniques, and applications, 3rd ed, A John Willey and Sons. Inc. Publication, Canada. https://doi.org/10.1016/0021-8502(80)90037-3

Bauer, S.E., Menon, S., Koch, D., Bond, T.C., Tsigaridis, K., 2010. A global modeling study on carbonaceous aerosol microphysical characteristics and radiative effects. Atmos. Chem. Phys. 10, 7439–7456. https://doi.org/10.5194/acp-10-7439-2010

Beresford, N.A., Scott, E.M., Copplestone, D., 2019. Field effects studies in the Chernobyl exclusion zone: Lessons to be learnt. J. Environ. Radioact. 1–10. https://doi.org/10.1016/j.jenvrad.2019.01.005

Bond, T.C., Doherty, S.J., Fahey, D.W., Forster, P.M., Berntsen, T., Deangelo, B.J., Flanner, M.G., Ghan, S., Kärcher, B., Koch, D., Kinne, S., Kondo, Y., Quinn, P.K., Sarofim, M.C., Schultz, M.G., Schulz, M., Venkataraman, C., Zhang, H., Zhang, S., Bellouin, N., Guttikunda, S.K., Hopke, P.K., Jacobson, M.Z., Kaiser, J.W., Klimont, Z., Lohmann, U., Schwarz, J.P., Shindell, D., Storelvmo, T., Warren, S.G., Zender, C.S., 2013. Bounding the role of black carbon in the climate system: A scientific assessment. J. Geophys. Res. Atmos. 118, 5380–5552. https://doi.org/10.1002/jgrd.50171

Chen, K., Yin, Y., Kong, S., Xiao, H., Wu, Y., Chen, J., Li, A., 2014. Size-resolved chemical composition of atmospheric particles during a straw burning period at Mt. Huang (the Yellow Mountain) of China. Atmos. Environ. 84, 380–389. https://doi.org/10.1016/j.atmosenv.2013.11.040

Chen, Y., Bond, T.C., 2010. Light absorption by organic carbon from wood combustion. Atmos. Chem. Phys. 10, 1773–1787. https://doi.org/10.5194/acp-10-1773-2010

Chen, Z., Chen, X., Zheng, Y., Sun, J., Chen, F., Shi, L., Li, F., Dong, Y., Zhang, Z., 2017. Air ingress analysis of chimney effect in the 200 MWe pebble-bed modular high temperature gas-cooled reactor. Ann. Nucl. Energy 106, 143–153. https://doi.org/10.1016/j.anucene.2017.03.041

Cheng, Y.F., Berghof, M., Garland, R.M., Wiedensohler, A., Wehner, B., Müller, T., Su, H., Zhang, Y.H., Achtert, P., Nowak, A., Poschl, U., Zhu, T., Hu, M., Zeng, L.M.,

2009. Influence of soot mixing state on aerosol light absorption and single scattering albedo during air mass aging at a polluted regional site in northeastern China. J. Geophys. Res. Atmos. 114, 1–20. https://doi.org/10.1029/2008JD010883

Chi, S.H., Chan Kim, G., 2017. Effects of air flow rate on the oxidation of NBG-18 and NBG-25 nuclear graphite. J. Nucl. Mater. 491, 37–42. https://doi.org/10.1016/j.jnucmat.2017.04.032

Contescu, C.I., Azad, S., Miller, D., Lance, M.J., Baker, F.S., Burchell, T.D., 2008. Practical aspects for characterizing air oxidation of graphite. J. Nucl. Mater. 381, 15–24. https://doi.org/10.1016/j.jnucmat.2008.07.020

Contescu, C.I., Guldan, T., Wang, P., Burchell, T.D., 2012. The effect of microstructure on air oxidation resistance of nuclear graphite. Carbon N. Y. 50, 3354–3366. https://doi.org/10.1016/j.carbon.2012.01.040

Dayan, A., Paine, A.J., 2001. Mechanisms of chromium toxicity, carcinogenicity and allergenicity: Review of the literature from 1985 to 2000. Hum. Exp. Toxicol. 20, 439–451. https://doi.org/10.1191/096032701682693062.

Deuerling, C.F., Maguhn, J., Nordsieck, H.O., Warnecke, R., Zimmermann, R., 2010. Measurement system for characterization of gas and particle phase of high temperature combustion aerosols. Aerosol Sci. Technol. 44, 1–9. https://doi.org/10.1080/02786820903325402

Du, Y., Gao, B., Zhou, H., Ju, X., Hao, H., Yin, S., 2013. Health risk assessment of heavy metals in road dusts in urban parks of Beijing, China. Procedia Environ. Sci. 18, 299–309. https://doi.org/10.1016/j.proenv.2013.04.039

Dulera, I. V., Sinha, R.K., 2008. High temperature reactors. J. Nucl. Mater. 383, 183–188. https://doi.org/10.1016/j.jnucmat.2008.08.056

Dulera, I. V., Sinha, R.K., Rama Rao, A., Patel, R.J., 2017. High temperature reactor technology development in India. Prog. Nucl. Energy 101, 82–99. https://doi.org/10.1016/j.pnucene.2017.04.020

Englert, M., Frieß, F., Ramana, M. V., 2017. Accident scenarios involving pebble bed high temperature reactors. Sci. Glob. Secur. 25, 42–55. https://doi.org/10.1080/08929882.2017.1275320

Fachinger, J., 2012. Graphite. Compr. Nucl. Mater. 5, 539–561. https://doi.org/10.1016/B978-0-08-056033-5.00110-5

Fallis, A.., 2013. Climate change and nuclear power. J. Chem. Inf. Model. 53, 1689–1699. https://doi.org/10.1017/CBO9781107415324.004

Fang, G.C., Chang, C.N., Wu, Y.S., Wang, V., Fu, P.P.C., Yang, D.G., Chen, S.C., Chu, C.C., 2000. The study of fine and coarse particles, and metallic elements for the daytime and night-time in a suburban area of central Taiwan, Taichung. Chemosphere 41, 639–644. https://doi.org/10.1016/S0045-6535(99)00507-X

Feng, T., Li, H.J., Hu, M.H., Lin, H.J., Li, L., 2016. Oxidation and ablation resistance of Fe 2 O 3 modified ZrB_2 –SiC–Si coating for carbon/carbon composites. Ceram. Int. 42, 270–278. https://doi.org/10.1016/j.ceramint.2015.08.105

Fermi, E., 1952. Experimental production of a divergent chain reaction. Am. J. Phys. 20, 536–558. https://doi.org/10.1119/1.1933322

Ferng, Y.M., Chi, C.W., 2012. CFD investigating the air ingress accident for a HTGR simulation of graphite corrosion oxidation. Nucl. Eng. Des. 245, 28–38. https://doi.org/10.1016/j.nucengdes.2012.03.041

Glytsos, T., Ondrá, J., Dzumbova, L., Kopanakis, I., Lazaridis, M., 2010. Characterization of particulate matter concentrations during controlled indoor activities. Atmos. Environ. 44, 1539–1549. https://doi.org/10.1016/j.atmosenv.2010.01.009

Gupta, S., Kanzleiter, T., Fischer, K., Poss, G., 2010. Reactor safety research program at THAI test facility, in: 17th Pacific basin nuclear conference Cancún, Q.R., México. pp. 1–19.

Hansen, J., Sato, M., Ruedy, R., Lacis, A., Oinas, V., 2000. Global warming in the twenty-first century: An alternative scenario. Proc. Natl. Acad. Sci. U. S. A. 97, 9875–9880. https://doi.org/10.1073/pnas.170278997

Hinssen, H.K., Katscher, W., Moormann, R., 1983. Kinetics of the graphite/oxygen reaction in the in-pore diffusion controlled regime. Pt. 1 (Juel--1875). Germany.

Hishida, M., Takeda, T., 1991. Study on air ingress during an early stage of a primary-pipe rupture accident of a high-temperature gas-cooled reactor. Nucl. Eng. Des. 126, 175–187. https://doi.org/10.1016/0029-5493(91)90109-U

Hu, X., Zhang, Y., Ding, Zhuhong WangHongzhen, T., Lian, H., Sun, Y., Wu, J., 2012. Bioaccessibility and health risk of arsenic and heavy metals (Cd, Co, Cr, Cu, Ni, Pb,Zn and Mn) in TSP and PM2.5 in Nanjing, China. Atmos. Environ. 57, 146–152.

Huang, L., Lin, W., Li, F., Wang, Y., Jiang, B., 2019. Climate impacts of the biomass burning in Indochina on atmospheric conditions over Southern China. Aerosol Air Qual. Res. 19, 2707–2720. https://doi.org/10.4209/aaqr.2019.01.0028

Huang, W.H., Tsai, S.C., Chiu, I.C., Chen, C.H., Kai, J.J., 2014. The oxidation effects of nuclear graphite during air-ingress accidents in HTGR. Nucl. Eng. Des. 271, 270–274. https://doi.org/10.1016/j.nucengdes.2013.11.047

IAEA, 2001. Current status and future development of modular high temperature gas cooled reactor technology (IAEA-TECDOC-1198).

Jacobson, M.Z., 2010. Short-term effects of controlling fossil-fuel soot, biofuel soot and gases, and methane on climate, Arctic ice, and air pollution health. J. Geophys. Res. Atmos. 115. https://doi.org/10.1029/2009JD013795

Jacobson, Z., 2000. Implications for global direct forcing of aerosols well-mixed. October 27, 217–220.

Jaishankar, M., Tseten, T., Anbalagan, N., Mathew, B.B., Beeregowda, K.N., 2014. Toxicity, mechanism and health effects of some heavy metals. Interdiscip. Toxicol. 7, 60–72. https://doi.org/10.2478/intox-2014-0009

Jiang, X.Q., Mei, X.D., Feng, D., 2016. Air pollution and chronic airway diseases: What should people know and do? J. Thorac. Dis. 8, E31–E40. https://doi.org/10.3978/j.issn.2072-1439.2015.11.50

Kadak, A.C., Zhai, T., 2006. Air ingress benchmarking with computational fluid dynamics analysis. Nucl. Eng. Des. 236, 587–602. https://doi.org/10.1016/j.nucengdes.2005.11.019

Kane, J.J., Contescu, C.I., Smith, R.E., Strydom, G., Windes, W.E., 2017a. Understanding the reaction of nuclear graphite with molecular oxygen: Kinetics, transport, and structural evolution. J. Nucl. Mater. 493, 343–367. https://doi.org/10.1016/j.jnucmat.2017.06.001

Kane, J.J., Contescu, C.I., Smith, R.E., Strydom, G., Windes, W.E., 2017b. Understanding the reaction of nuclear graphite with molecular oxygen: Kinetics, transport, and structural evolution. J. Nucl. Mater. 493, 343–367. https://doi.org/10.1016/j.jnucmat.2017.06.001

Kelly, C., 2016. Scientists discuss complexities of studying tiny particles that have a big impact on climate. phys.org. URL https://phys.org/news/2016-03-scientists-discuss-complexities-tiny-particles.html

Kirchstetter, T.W., Novakov, T., Hobbs, P. V., 2004. Evidence that the spectral dependence of light absorption by aerosols is affected by organic carbon. J. Geophys. Res. D Atmos. 109, 1–12. https://doi.org/10.1029/2004JD004999

Koch, D., Del Genio, A.D., 2010. Black carbon semi-direct effects on cloud cover: Review and synthesis. Atmos. Chem. Phys. 10, 7685–7696. https://doi.org/10.5194/acp-10-7685-2010.

Kugeler, K., Epping, C., Schmidtlein, P., Schreiner, P., 1992. Aerosol formation by graphite corrosion in case of water and air ingress to the core of a high-temperature reactor. Nucl. Eng. Des. 137, 213–219. https://doi.org/10.1016/0029-5493(92)90020-V

Levenspiel, O., 1964. Chemical reaction engineering, Chemical Engineering Science. https://doi.org/10.1016/0009-2509(64)85017-X

Li, L., Li, H., Shen, Q., Lin, H., Feng, T., Yao, X., Fu, Q., 2016. Oxidation behavior and microstructure evolution of SiC-ZrB_2 -ZrC coating for C/C composites at 1673 K. Ceram. Int. 42, 13041–13046. https://doi.org/10.1016/j.ceramint.2016.05.083

Liu, J., Dong, L., Wang, C., Liang, T., Lai, W., 2015. First principles study of oxidation behavior of irradiated graphite. Nucl. Instruments Methods Phys. Res. Sect. B Beam Interact. with Mater. Atoms 352, 160–166. https://doi.org/10.1016/j.nimb.2014.12.071.

Loren Fuller, E., Okoh, J.M., 1997. Kinetics and mechanisms of the reaction of air with nuclear grade graphites: IG-110. J. Nucl. Mater. 240, 241–250. https://doi.org/http://dx.doi.org/10.1016/S0022-3115(96)00462-X

Makino, A., Kato, I., Senba, M., Fujizaki, H., Araki, N., 1996. Flame structure and combustion rate of burning graphite in the stagnation flow. Symp. Combust. 26, 3067–3069. https://doi.org/10.1016/S0082-0784(96)80150-0

Mancuso, T.., 1975. International Conference on Heavy Metals in the Environment. Consid. Chromium as an Ind. Carcinog.

Masoudifar, S., Bavand-Vandchali, M., Golestani-Fard, F., Nemati, A., 2016. Molten salt synthesis of a SiC coating on graphite flakes for application in refractory castables. Ceram. Int. 42, 11951–11957. https://doi.org/10.1016/j.ceramint.2016.04.120

McConnell, J.R., Edwards, R., Kok, G.L.., Flanner, M.G.., Zender, C.S., Saltzman, E.S.., 2007. 20th-Century industrial black carbon emissions altered arctic climate forcing. Science (80-.). 317, 1381–1385.

Ming, J., Cachier, H., Xiao, C., Qin, D., Kang, S., Hou, S., Xu, J., 2008. Black carbon record based on a shallow Himalayan ice core and its climatic implications. Atmos. Chem. Phys. 8, 1343–1352. https://doi.org/10.5194/acp-8-1343-2008

Moormann, R., 2011. Phenomenology of graphite burning in air ingress accidents of HTRs. Sci. Technol. Nucl. Install. 2011, 13. https://doi.org/10.1155/2011/589747.

Mukherjee, S., Roychoudhury, S., Siddique, S., Banerjee, M., Bhattacharya, P., Lahiri, T., Ray, M.R., 2014. Respiratory symptoms, lung function decrement and chronic obstructive pulmonary disease in pre-menopausal Indian women exposed to biomass smoke. Inhal. Toxicol. 26, 866–872. https://doi.org/10.3109/08958378.2014.965560

Nechepurenko, A., Samuni, S., 2000. Oxidation protection of graphite by BN coatings. J. Solid State Chem. 154, 162–164. https://doi.org/10.1006/jssc.2000.8829

Park, S.J., 2018. Carbon/carbon composites. Springer Ser. Mater. Sci. 210, 279–294. https://doi.org/10.1007/978-981-13-0538-2_8

Peng, L., Zhipeng, C., Yanhua, Z., Jun, S., Fubing, C., Lei, S., Fu, L., Yujie, D., Zuoyi, Z., 2016. Study on air ingress of the 200 MWe pebble-bed modular high temperature gas-cooled reactor. Ann. Nucl. Energy 98, 120–131. https://doi.org/10.1016/j.anucene.2016.07.029

Proctor, D.M., Suh, M., Campleman, L.S., Thompson, C.M., 2014. Assessment of the mode of action for hexavalent chromimum- induced lung cancer following inhalation exposures. Toxicology 325, 160–179.

Peng, W., Changling, Z., Xinghong, Z., Guangdong, Z., Baosheng, X., Yehong, C., Peng, Z., Wenbo, H., 2016. Oxidation protective ZrB_2-SiC coatings with ferrocene addition on SiC coated graphite. Ceram. Int. 42, 2654–2661. https://doi.org/http://dx.doi.org/10.1016/j.ceramint.2015.10.072

Propp, W.A., 1998. Graphite Oxidation Thermodynamics/Reactions. Other Inf. PBD 1 Sep 1998 35.

Ramanathan, V., Carmichael, G., 2008. Global and regional climate changes due to black carbon. Nat. Geosci. 1, 221–227. https://doi.org/10.1038/ngeo156

Remiarova, B., Markos, J., Zajdlik, R., Jelemensky, L., 2004. Identification of the mechanism of coal char particle combustion by porous structure characterization. Fuel Process. Technol. 85, 303–321.

Riemer, N., Ault, A.P., West, M., Craig, R.L., Curtis, J.H., 2019. Aerosol Mixing State: Measurements, Modeling, and Impacts. Rev. Geophys. 57, 187–249. https://doi.org/10.1029/2018RG000615

Rush, H.J., MacKerron, G., Surrey, J., 1977. The advanced gas-cooled reactor. Energy Policy 5, 95–105. https://doi.org/10.1016/0301-4215(77)90003-9

Schweitzer, D.G., 1962. Oxidation and Heat Transfer Studies in Graphite Channels: IV. Combined Effects of Temperature, Flow Rate, Diameter, and Chemical Reactivity on the Length of Channel Cooled by Air. Nucl. Sci. Eng. 12, 59–62. https://doi.org/10.13182/nse62-a25370

Singla, V., Mukherjee, S., Kashikar, A.S., Safai, P.D., Pandithurai, G., 2019. Black carbon: source apportionment and its implications on CCN activity over a rural region in Western Ghats, India. Environ. Sci. Pollut. Res. 26, 7071–7081. https://doi.org/10.1007/s11356-019-04162-w

Spracklen, D. V., Carslaw, K.S., Pöschl, U., Rap, A., Forster, P.M., 2011. Global cloud condensation nuclei influenced by carbonaceous combustion aerosol. Atmos. Chem. Phys. 11, 9067–9087. https://doi.org/10.5194/acp-11-9067-2011

Stanculescu, A., 2010. Fast Reactor Technology Development Activities.

Thanh, N.T.K., Maclean, N., Mahiddine, S., 2014. Mechanisms of nucleation and growth of nanoparticles in solution. Chem. Rev. 114, 7610–7630. https://doi.org/10.1021/cr400544s

The U.S. Department of energy, 2010. Next generation nuclear plant (NGNP) U.S_2010.

Theodosiou, A., Jones, A., Marsden, B., 2017. Thermal oxidation of nuclear graphite: A large scale waste treatment option. PLoS One 12, 1–19. https://doi.org/10.7910/DVN/ANVCDX.

Tiwari, M., Sahu, S.K., Bhangare, R.C., Yousaf, A., Pandit, G.G., 2014. Particle size distributions of ultrafine combustion aerosols generated from household fuels. Atmos. Pollut. Res. 5, 145–150. https://doi.org/10.5094/APR.2014.018.

Toll, V., Christensen, M., Quaas, J., Bellouin, N., 2019. Weak average liquid-cloud-water response to anthropogenic aerosols. Nature 572, 51–55. https://doi.org/10.1038/s41586-019-1423-9

Von Der Weiden, S.L., Drewnick, F., Borrmann, S., 2009. Particle Loss Calculator - A new software tool for the assessment of the performance of aerosol inlet systems. Atmos. Meas. Tech. 2, 479–494. https://doi.org/10.5194/amt-2-479-2009.

Wang, L., Wang, Y., Du, H., Zuo, J., Li, R.Y.M., Zhou, Z., Bi, F., Garvlehn, M.P., 2019. A comparattive life- cycle assessment of hydro-, nuclear and wind power: A China study. Appl. Energy 249, 37–45.

Wang, P., Zhou, S., Hu, P., Chen, G., Zhang, X., Han, W., 2016. Ablation resistance of ZrB_2-SiC/SiC coating prepared by pack cementation for graphite. J. Alloys Compd. 682, 203–207. https://doi.org/10.1016/j.jallcom.2016.04.010.

Wang, Q., Li, Y., Luo, M., Sang, S., Zhu, T., Zhao, L., 2014. Strengthening mechanism of graphene oxide nanosheets for Al_2O_3-C refractories. Ceram. Int. 40, 163–172. https://doi.org/10.1016/j.ceramint.2013.05.117.

WHO, 2005. Indoor air pollution and health

William C. Hinds, 1999. Aerosol technology properties behavior and measurement of Airborne Particles, 2nd ed, A Wiley-Interscience Publication John Wiley & Sons, Inc. https://doi.org/10.1533/9781845695750.frontmatter.

Wu, Z., Lin, D., Zhong, D., 2002. The design features of the HTR-10. Nucl. Eng. Des. 218, 25–32. https://doi.org/10.1016/S0029-5493(02)00182-6.

Xiaowei, L., Jean-Charles, R., Suyuan, Y., 2004. Effect of temperature on graphite oxidation behavior. Nucl. Eng. Des. 227, 273–280. https://doi.org/10.1016/j.nucengdes.2003.11.004.

Xu, W., Sun, J., Zheng, Y., Shi, L., 2017. The influence of nuclear graphite oxidation on air ingress accident of HTR-PM. Ann. Nucl. Energy 110, 1242–1248. https://doi.org/10.1016/j.anucene.2017.08.028.

Xu, X., Li, Y., Wang, Q., Sang, S., Pan, L., 2017. Effect of alumina-coated graphite (ACG) on the microstructure and mechanical properties of Al_2O_3-C refractories. J. Ceram. Sci. Technol. 8, 455–462. https://doi.org/10.4416/JCST2016-00079.

Yagi, S., Kunii, D., 1961. Fluidized-solids reactors with continuous solids feed-I. Residence time of particles in fluidized beds. Chem. Eng. Sci. 16, 364–371. https://doi.org/10.1016/0009-2509(61)80043-2.

Yang, X., Zhao-hui, C., Feng, C., 2014. Journal of Asian Ceramic Societies High-

temperature protective coatings for C / SiC composites. Integr. Med. Res. 2, 305–309. https://doi.org/10.1016/j.jascer.2014.07.004.

Yuan, X., Zuo, J., Ma, R., Wang, Y., 2017. How would social acceptance affect nuclear power plant development? A study from china. J. Clean. Prod. 163, 179–186.

Zajdlik, R., Jelemensky, L., Remiarova, B., Markos, J., 2001. Experimental and modelling investigations of single coal particle combustion. Chem. Eng. Sci. 56, 1355–1361. https://doi.org/10.1016/S0009-2509(00)00358-4

Zhang, S., Lee, W.E., 2003. Improving the water-wettability and oxidation resistance of graphite using Al2O3/SiO2 sol-gel coatings. J. Eur. Ceram. Soc. 23, 1215–1221. https://doi.org/10.1016/S0955-2219(02)00284-4

Zhang, Y., Bai, Y., Jia, J., Gao, N., Li, Y., Zhang, R., Jiang, G., Yan, B., 2014. Perturbation of physiological systems by nanoparticles. Chem. Soc. Rev. 43, 3762–3809. https://doi.org/10.1039/c3cs60338e

Zheng, Y., Stempniewicz, M.M., 2012. Investigation of NACOK air ingress experiment using different system analysis codes. Nucl. Eng. Des. 251, 423–432. https://doi.org/10.1016/j.nucengdes.2011.09.050

Zhou, X.W., Yang, Y., Song, J., Lu, Z.M., Liu, B., Tang, Y.P., 2018. Carbon materials in a high temperature gas - cooled reactor pebble- bed module. New Carbon Mater. 33, 97–108.